Article

JOURNAL OF COMPOSITE MATERIALS

Journal of Composite Materials
2023, Vol. 57(5) 913–928

DOI: 10.1177/00219983221147381
journals.sagepub.com/home/jcm
SAGE

Extraction and characterization of novel natural fiber from Centaurea melitensis plant

Abd Raouf KHALDOUNE[1,2] and Mansour ROKBI[1]

Abstract

In this work a new cellulosic fibers extracted from *Centaurea Melitensis* plant to the prospect of employing them as a source of reinforcement in composite materials. In this investigation, morphological, chemical, physical and mechanical features of *Centaurea Melitensis* fibers are investigated. The morphological characteristics using anatomical technique and scanning electron microscopy revealed the presence of a large percentage of fibroblasts in the fibers that allow adhesion with the matrix when manufacturing of composite materials. The fiber density is 1.269 ± 0.018 g/cm^3 and the diameter is 187.11 ± 60.41 μm depending on the physical properties. The chemical properties revealed that the *Centaurea Melitensis* fiber has a crystalline size of 16.92 nm and a crystallinity index of 47.69% using XRD. The results of FTIR analysis proved on major components such as cellulose, hemicelluloses and lignin, by TGA the thermal stability was found up to 210°C and the maximum temperature up to 317.86°C. The mechanical properties have shown that the value of the tensile strength of the fibers is 336.87 ± 59.94 MPa, Young's modulus is 23.87 ± 5.21 GPa, and the strain at failure is 1.27 ± 0.36%, and the interfacial shear strength is 9.82 ± 2.35 MPa. The statistical approach, Weibull distribution was used with two and three parameters to examine the experimental data due to their dispersion. WEIBULL statistical analytical test was used with 2 and 3 parameters are used to examine the experimental data due to their dispersion. All the findings from this investigation reveal that *Centaurea Melitensis* fibers can be a qualified candidate to be used as reinforcement in low density composite materials.

Keywords

Centaurea melitensis, lignocellulosic, anatomical technique, ATR-FTIR, thermo gravimetric analysis, XRD, mechanical test

Introduction

Many research studies are now focusing on biodegradable, non-toxic, and renewable materials mainly motivated by the continuous decrease of fossil fuels and climate changes in environmental concerns.[1] On the other hand, the traditional materials such as carbon fibers, glass fibers, and aramid fibers, are known as carcinogenic materials after extended exposure.[2] For example, exposure to glass fibers showed DNA damage due to oxidative stress after exposure to high concentrations of fiberglass particles.[3] Additionally, increased eosinophils activators cause a decrease in blood lymphocytes and sensitivity.[4] In others words, Glass fiber workers are exposed to stimulation of T-cells and B-cells, which causes inhibition of lymhocytes in the blood, which leads to an increases in the secretion of eosinophils that lead to allergic reactions in fiber glass workers. On the other hand, according to various studies, natural fibers can offer several advantages over synthetic fibers such as biodegradability, cost effectiveness extraction, less hazardous manufacturing method, low density, non-polluting nature, and low specific strength dependent on texture and water. Furthermore natural fibers exhibit natural characteristics and improved insulation.[5] This technical advancement and the inherent natural characteristics of natural fibers have motivated scientists to go further in their research in order to improve their qualities and produce eco-friendly and affordable goods.[6]

Natural fibers are increasingly being used in the creation of composite materials, notably in construction, sports

[1]Department of Mechanical Engineering, Faculty of Technology, University of M'sila, M'sila, Algeria
[2]Laboratoire de Matériaux et Mécanique des Structures (LMMS), University of M'sila, M'sila, Algeria

Corresponding author:
Mansour Rokbi, Department of Mechanical Engineering , University of M'sila, University pole of M'sila, Algeria.
Email: mansour.rokbi@univ-msila.dz

equipment, vehicles, aircraft, marine, household appliances, textiles, and other equipment in other areas.[7] In the literature referred to the extraction of natural fibers several techniques has been mentioned. However it is worth mentioning that plant elements such as the stem, root, fruit, leaves, and bark influence the used extraction procedures (biological, chemical, or mechanical) which affect the fiber quality and performance.[8] It is worth noting that natural fibers consist mostly of cellulose, hemicelluloses, and non-cellulose ingredients such as pectin and wax. The proportions of these components are largely determined by plant species, age, and organs.[9] The various investigations on the characterization of novel cellulosic fibers, aim mainly to use it as a component in composite materials. For instance *Siva, R., et al*[10] analyzed *Kigelia africana* fibers and found the ratio of density of 1.316 g/cm^3 fibers that helps to use them in lightweight structural applications. It was also noted from the results of Thermal Gravimetric Analysis (TGA) that thermal stability ratio reaches 212°C, which ensures the appropriateness of its use in composite materials. *Chakravarthy, S., et al*[11] described the *Cissus vitiginea stem* fiber where it is found that the crystallinity index of 30.5% and a crystallization size ratio of 12.69 nm, indicating that the fibers contain a large proportion of cellulose. They also tested the single fiber tensile with *a gauge length* GL = 40 mm and found the tensile strength of 304.43 ± 35 MPa, Young's modulus of 5.85 ± 1.10 GPa, and strain at failure of 8.92 ± 1.4%. Other recent works have focused their investigations on recently found natural fibers from *Momordica charantia,*[12] *Cereus Hildmannianus,*[13] *Vachellia farnesiana,*[14] *Cardiospermum Halicababum,*[15] *Silybum marianum,*[16] and *Areca catechu L*[17] in order to address growing industrial demands that aren't being supplied entirely by present cellulosic fiber production.[18]

This research focuses on the investigation of fibers extracted from *Centaurea Melitensis* plant which is an annual prickly plant endemic to the mediterranean region that belongs to the Asteraceae family. Although it has been introduced in many regions in the world, but it is especially invasive in mediterranean temperature zones, reaching a height of 85 cm and spreading in grasslands, disturbed areas, and roadside areas.[19] In addition, several Centaurea species (Asteraceae) have been identified as aggressive invaders.[20] After winter rains, *Centaurea Melitensis* begins to grow in early spring and flowers in late spring and early summer.[21] Invasive species use more resources for development and reproduction than native plants, according to studies of *Centaurea Melitensis*, *Centaurea solstitialis*, and *Centaurea stoebe*.[22] Although *Centaurea Melitensis* is a demanded plant in many areas, it is still not economically valuable.[23] *Centaurea Melitensis* fibers, in this sense, could be the best useful option for making composite materials regarding their widespread availability and abundance.

In the present work, a new cellulosic fiber that is extracted from the *Centaurea Melitensis* plant is investigated to verify the possibility to be used as a reinforcement in bio-composite. Indeed, in this investigation, the morphologic, chemistry, physical and mechanical features were examined. The physical features (density)were verified using Pycnometer technique. While anatomy technique is used to identify morphological details of the plant. In chemical features extraction the fiber samples were examined using a ATR-FTIR equipment to guarantee the existence of the major components and XRD to determine the crystallization index. Regarding thermal parameters, such as thermal stability and pyrolysis temperature of the polymerization temperature tolerance, were investigated using TGA. On the other hand, the single fiber tensile test and WEIBULL statistical analysis were used to determine the mechanical behavior. Finally, Scanning Electron Microscopy (SEM) was used to examine the morphology of the plant surface. The main and major contribution in this research work is the characterization and features extraction of a new fiber, suitable for composite materials, obtained from *Centaurea Melitensis (CM)* plant which is an abundant and cost effective plant. And it has two important aspects, the first interesting aspect is that the fibers used in this research are abundant in nature, which facilitates the production of composite materials. The second novelty is that the fibers have suitable properties in the production of lightweight structures.

Materials and experimental procedure

Plant material

The fibers used in this study were collected from *Centaurea Melitensis* plant. This last is found in the Hodna area of Algeria (35°42′7″N, 4°32′49″E, and 471m elevation). It grows naturally by the side of the road in Spring, reaching a height of around 85 cm and a diameter of 5–10 mm.

Fiber extraction

After harvesting the expected plant, basic steps are followed to extract the lignocellusic fibers from *Centaurea Melitensis stems*. Figure 1 shows the *CM* plant and the extracted fibers.

At first, *CM* stems are cleaned as well as dust contaminants and other unwanted foreign particles removed using distilled water. The stems are then submerged for 4 weeks in a tank filled with water tap water for bio-regeneration, allowing the fibers to separate from the stem.[24] The fibers were separated from the stems with a metal wire brush and washed with distilled water to extract them.

At the end of the procedure, the fibers are dried in an oven at 65°C for 6 h to reduce the amount of moisture. Figure 1(c), shows the obtained fibers using the aforementioned methodology.

Figure 1. *Centaurea Melitensis (CM)*: (a) plants, (b) stem, (c) extracted fibers.

Characterization methods

Anatomical technique. In order to study and investigate the internal structure of *CM* plant, an anatomical study was performed. A sharp razor blade was used to cut the stems into small 0.5 mm pieces. After the cross-sections were soaked in sodium hypochlorite solution (bleach) and then they were washed thoroughly with distilled water. After that, a short washing is performed in dilute acetic acid, followed by a wash with distilled water. The final pieces were then cleaned with distilled water after immersing them in carmine green iodine. Before being examined with a microscope (OPTIKA B-350), samples are carefully inserted between the slide and the cap.

Density measurement. The density of the fibers (ρ_f) is evaluated using Pycnometer technique. To this end, the Pycnometer is filled with a liquid called Ethanol where its density is $\rho_e = 0.79$ g/cm^3. Before performing density measurement, a sample of the fiber is subdivided into small pieces of 10 mm. Then, the overall pieces are dried in an oven at 90°C for 20 min. Finally, about 1 g of the fiber is immersed in Ethanol and the measurements were conducted with a sensitivity scale of 0.0001 g. The fiber density was obtained using the following expression

$$\rho_f = \frac{(m_2 - m_0)}{(m_1 - m_0) - (m_3 - m_2)}\rho_e \quad (1)$$

where
m_0 stands for the mass of the unfilled Pycnometer, m_1 stands for the mass of the ethanol-filled Pycnometer, m_2 stands for the mass of the combined Pycnometer and fibers, and m_3 stands for the mass of the Pycnometer filled with ethanol and fibers.

The area of the cross-section was estimated using the formula[25]

$$S_f = \frac{M}{\rho_f * L} \quad (2)$$

where
S_f stands for the cross section area of the fiber, M is the mass of the fiber, L stands for the fiber length and ρ_f stands for the fiber density.

Assuming a cylindrical form of the fiber and using the density the expressions given in equations (1) and (2), the equivalent diameter is calculated using the following relationship.[26]

$$D_e(\mu m) = \sqrt{4 * D(mtex)/\pi.\rho_f(g/cm^3)} \quad (3)$$

ATR-FTIR analysis. The elements of the functional group present in the composition of the *CM* fibers are determined using ATR-FTIR. The test process using FTIR is carried out at a room temperature using Cary630KBr apparatus from Agilent Technologies. Infrared spectrum is recorded with a spectral resolution of 2 cm^{-1} in the wavelength range between the field of 4000 cm^{-1} and 400 cm^{-1}.

TGA. The study and analysis of the Thermal Gravimetric (TGA) on *CM* fibers is performed using (SDT Q600 V20.9 Build device). Actually, the test is performed as follows: 6 mg of *CM* powder has been placed in trumpet alumina and inserted in an oven with a controlled atmosphere where the rate of nitrogen flow is of 20 mL/min.

The temperature range can be varied from ambient temperature (i.e. room temperature) to a level of temperature that can reach 600°C, with an average heating temperature of 10°C per minute.

XRD. Analytical XRD Analysis technique allows crystallization (CI) of *CM* fibers to be carried out by an X-ray diffraction diagnostic device "BRUKER D8" with Cu- Kα (Kα = 1.54,056), while maintaining the spectra range between 10° and 70° (Field Angle 2θ). The XRD is fixed at 40 kV and 30 mA and the crystallinity index (CI) is calculated by the empirical relationship given by expression (4) formulated by reference [27]:

$$CI\% = \frac{(I_{002} - Iam)}{\mathrm{I}_{002}} \times 100 \quad (4)$$

where
I_{002} represents the crystalline peak's greatest intensity at (2θ = 22), and I_{am} represents the amorphous peak's (minimum) intensity at (2θ = 16.86) respectively. Scherrer's equation was also used to estimate the crystallite size (CS)[11]

$$CS = \frac{k\lambda}{\beta coc\theta} \quad (5)$$

where
Scherrer's constant K = 0.89, λ stands for the spectrum wavelength in A°, β is the whole width of the peak in radians at half-maximum and θ is the diffraction angle.

Mechanical test. To determine the tensile properties of single fibers, the ASTM C1557-14 which is a method for testing the tensile properties of single fibers was used to determine the maximum tensile strength of *CM* fibers. The mechanical parameters (tensile strength, Young's modulus, and strain at fracture) were determined using the Zwick Roell test apparatus. The experiment was carried out with 30 single fibers, each having a gauge length of 40 mm, a transverse speed of 2.5 mm/min, and a load cell of 2.5 kN. It's worth mentioning that the most reliable findings are supplied.

Micro-droplet test. In this test, micro-drops are made by making knots with epoxy resin around *CM* fibers. This is a method that uses a thin metal rod to apply small drops of epoxy resin to individual fibers and then place them in a paper frame and leave to harden. Figure 2(a) shows the examination of droplet geometry using an optical microscope (MOTIC). Samples with defects, both in droplet and in fibers, are automatically rejected. Before testing, the paper frame is cut and tested on Instron ZWICK Z005 universal tensioning machine for micro-drop test on *CM* fiber. Figure 2(b) shows the method of placing the fibers on the device using two positioned blades. The blades are attached to the lower jaw of the Instron test system and the fibers are pulled through the upper jaw using a Phillips head speed of 0.5 mm/min. At least 10 samples were used for IFSS estimation and their average value was reported. Interfacial shear strength (IFSS) that determines the degree of adhesion in a given fibrous matrix system according to the following equation (6).[28]

$$\tau = IFSS = F_{max}/\pi dL \quad (6)$$

where τ is the interfacial shear strength (MPa), F_{max} is the maximum pull-out force; d is the fiber diameter and L is the embedded length.

Scanning electron microscopy. The outer surface of the *CM* fibers is examined using a scanning electron microscope Thermo scientific Quatro in a medium of high vacuum and low pressure.

Results and discussions

Anatomical technique

Figure 3 shows the microscopic view of an anatomical cross-section of *CM* stems. It is worth to highlight that the maturity of the plant plays an important role in determining the number of bundles and the size of the fibers.[29] In the studied case, the fibrous bundles appear evenly scattered throughout the epidermis. The epidermis and the Sclerenchyma can be

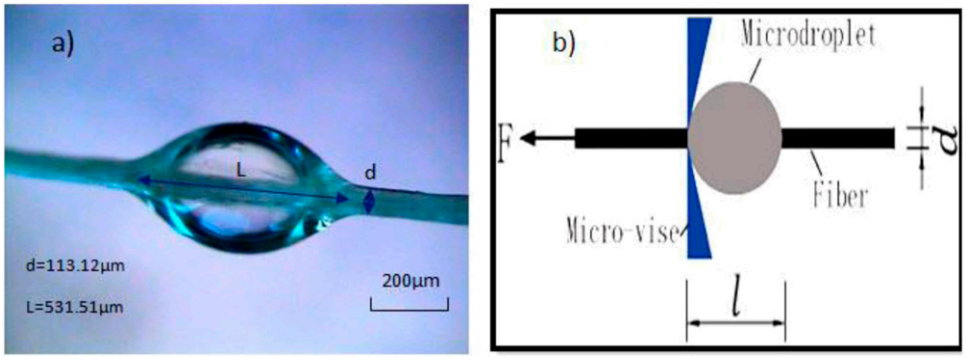

Figure 2. (a) Epoxy micro drop on individual *CM* fiber, (b) Droplet test of *CM* fiber.

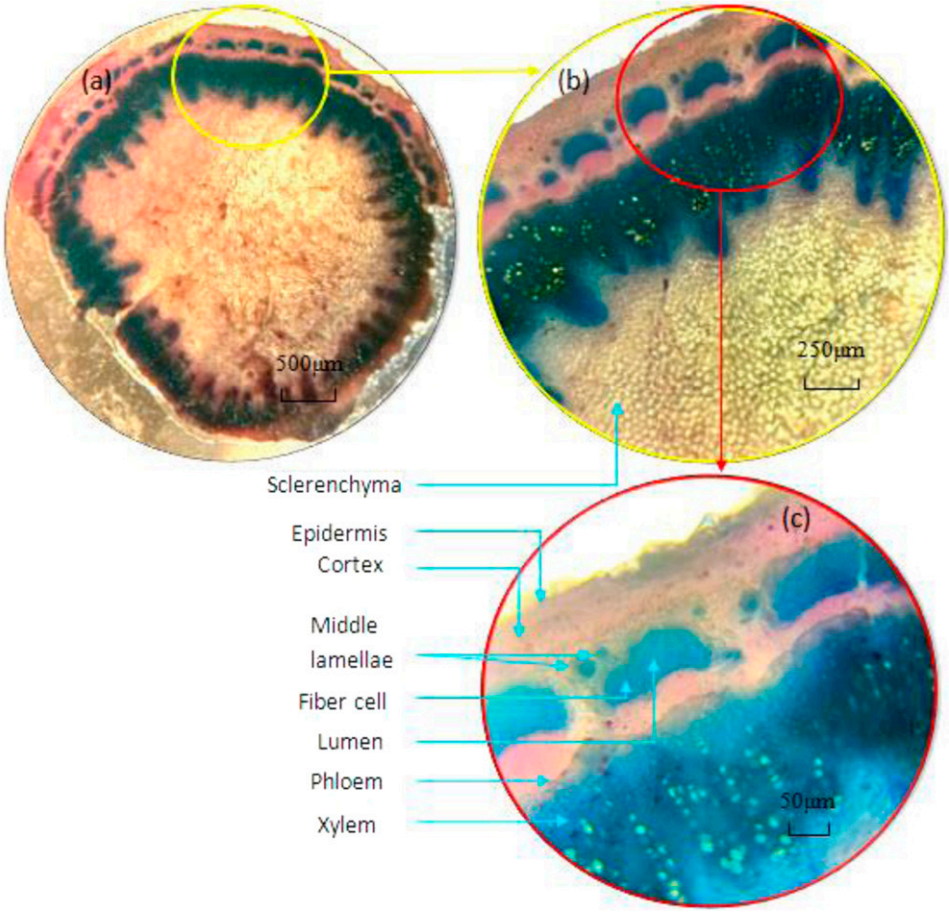

Figure 3. Microscopic view of *CM plant*: (a) Cross section, (b) and (c) Zoom view of the fiber cell structure.

viewed from the outside and the inside respectively (see Figure 3(a) and (b)) with the cellulose fibers connected in bundles by medial lamellae (see Figure 3(c)), phloem tubes and xylem in the middle. It forms a large number of fibroblasts in the composition of the fiber cells. The fiber cell is characterized by the presence of a primary cell wall followed by a secondary cell wall, with the lumen in the fiber center. Regarding the chemical structure of fiber cells, cellulose and lignin form the primary and secondary cell walls as lignin is a chemical substance that has the longest disintegration resistance, and the middle plate is made up of lignin and hemicelluloses.[30] This is why the fibroblasts' strength determines the fiber bundle's strength. In the center of the *stem*, vascular bundles are clearly apparent in Figure 3(c), where his substance is mostly made of xylem and phloem and is found adjacent to the bundle of fibers. This was previously reported in anatomical investigations on natural fibers by several researchers such as *Lygeum spartum L,*[29,31] *Silybum marianum,*[16] *Atriplex halimus L,*[32] *Strelitzia reginae.*[33]

Density measurement. Composite materials provide a greater weight-to-strength ratio, and are currently preferred for many lightweight structural parts since density is very important in determining the mass of natural fibers. Density analysis is performed as part of the characterization process for natural fibers. In this study the density value was obtained as 1.269 ± 0.018 g/cm^3 for *Centaurea Melitensis*. We notice that the density value was found to be lower than *Kigelia africana's* (1.316 g/cm^3), *Cissus vitiginea* stem (1.287 g/cm^3) and *Momordica charantia* (1.339 ± 0.0064 g/cm^3), *Cereus Hildmannianus* (1.364 ± 0.026 g/cm^3), and closer to *Vachellia farnesiana* fibers (1.270 ± 0.0048 g/cm^3). On the other hand we notice a greater value than *Cardiospermum Halicababum* fiber density (1.141 g/cm^3), *Silybum marianum* (1.098 g/cm^3), and *Areca catechu L* (0.75 ± 0.05 g/cm^3). As a result *Centaurea Melitensis* has a lower density than many other natural fibers, making it a better fit for current lightweight structural applications, including synthetic composite fiber constructions.[34] The density difference between natural fibers is caused by factors such as extraction processes, fiber porousness, and environmental conditions.[29] *Centaurea Melitensis* was estimated to have an average diameter of 187.11 ± 60.41 µm, which is comparable to that

of *Kigelia africana* (582 ± 204 µm) and *Cissus vitiginea stem* fibers (355.74 ± 16.43 µm), *Momordica charantia* fibers (198 ± 3.9 µm), *Cereus Hildmannianus* fibers (30.04 ± 5.72 µm), *Vachellia farnesiana* fibers (231 ± 2.68 µm), *Cardiospermum Halicababum* fibers (315.4 µm), *Silybum marianum* fibers (222 µm) and *Areca catechu L* fibers (395 ± 17 µm). Table 1 gives a comparison between the diameter and the density of *Centaurea Melitensis* to those reported for other natural fibers.

ATR–FTIR analysis

ATR-FTIR is greatly recommended to analyze the chemical structure of lignocellulosic fibers, in other words to identify the organic and polymeric compounds. Figure 4 shows the spectra obtained from FTIR investigation of *CM* fibers. They display patterns ranging from 4000 cm^{-1} to 500 cm^{-1}. The hydroxyl group and the O-H expansion vibration found in the polysaccharides cellulose and hemicelluloses are represented by the first absorption band, which is concentrated at wave number 3350 cm^{-1}.[35] Then, The prolonged vibration of CH in cellulose and hemicelluloses is represented by facet number 2884 cm^{-1}.[36] The H-O-H bending band has a peak at 1650 cm^{-1}, which was connected with absorbing water.[37] The C-C expansion maxima is obtained at 1600 cm^{-1} and 1500 cm^{-1} which indicate the existence of aromatic rings in lignin, respectively.[36] The expansion of CH_2 from cellulose is indicated by consecutive peaks at 1456 cm^{-1} and 1417 cm^{-1}.[38] The C-H expansion of lignin is shown by waves 1370 cm^{-1} and 1324 cm^{-1}.[35] The C = O expansion of the cholinergic groups reserved to an intense band at 1230 cm^{-1}.[39] The absorption band for the elongation of the C-O asymmetric cellulose bridge was 1153 cm^{-1}.[40] The asymmetric C-O-C bridge expanded in cellulose and hemicelluloses is responsible for the strong peak at 1029 cm^{-1}.[41] The last tiny peak intensity was seen at 897 cm^{-1}, which corresponds to the stretching band of β-glycoside bonds between monosaccharide's.[41] The

Table 1. Comparison of some physical properties of the *CM* fibers to other natural fibers.

Fibers type	Diameter (µm)	Density (g/cm^3)	References
Centaurea Melitensis	187.11 ± 60.41	1.269 ± 0.018	Present work
Kigelia africana	582 ± 204	1.316	10
Cissus vitiginea stem	355.74 ± 16.43	1.287	11
Momordica charantia	198 ± 3.9	1.339 ± 6.4	12
Cereus Hildmannianus	30.04 ± 5.72	1.364 ± 0.026	13
Vachellia farnesiana	231 ± 2.68	1.270 ± 4.48	14
Cardiospermum Halicababum	315.4	1.141	15
Silybum marianum	222	1.098	16
Areca catechu L	395 ±17	0.75 ± 0.05	17

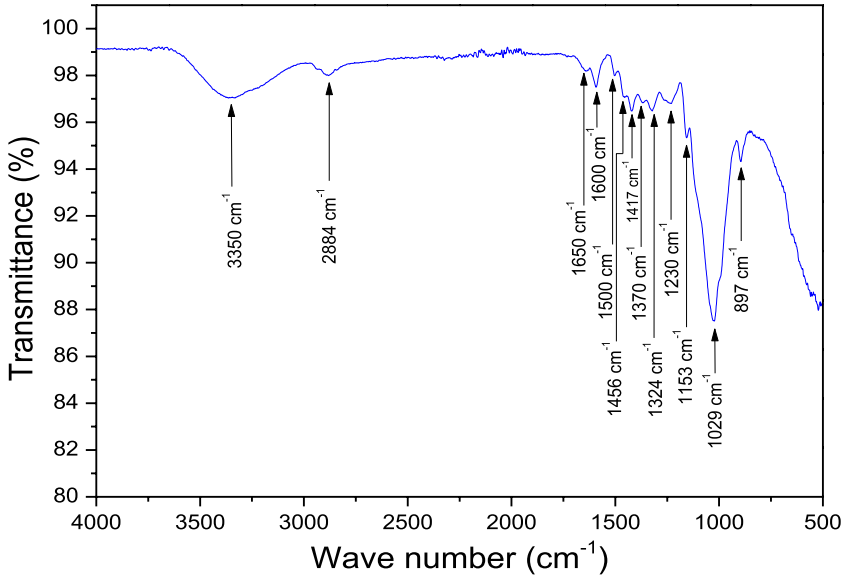

Figure 4. FTIR spectrum of the *CM* fibers.

reported values for FTIR domain differ from research to another research. The plant fiber bands' placements vary by roughly 16 cm^{-1}, and a single band might have many origins. As a result, band positions differ between investigations.[42] Peak wave numbers in the FTIR spectrum and chemical composition stretch assignment of *CM* are summarized in Table 2.

TGA

The TGA is a useful tool to evaluate the thermal behavior of lignocellulosic fibers. As known, the thermal properties of these materials are very crucial in manufacturing natural fiber composites to determine the best possible conditions for implementing of composites; and avoid the degradation of fiber properties.[43] In fact Standard Thermal Degradation curves for hemicelluloses, cellulose, and lignin characteristics are provided by thermo gravimetric analysis.[44] Figure 5 shown bellow, depicts a typical thermo gravimetric analysis and its derivatives from DTG curves for *CM* fibers.

The first step of disintegration in TGA occurs between 42°C −150°C, with a weight loss of 5.45%, indicating that water in the fibers has evaporated, proving that they are hydrophilic.[45] In thermo gravimetric study between 150 and 210°C, no weight loss was found, which may be used as a criteria in order to maintain the fibers thermal stability.[17] The second stage of degradation occurs between 210 and 330°C. Two major peaks can be seen in the second stage. The first peak occurs between 210 and 280°C, with a weight loss of 10.58%, indicating hemicelluloses hydrolysis and cellulose glycoside linkages hydrolysis.[29] The second peak occurs between 280 and 330°C with weight loss of 38.86% and a maximal rate of breakdown at 317.86°C with a weight loss of 54.89%. This rate of weight loss of most volatiles cellulose I and alpha cellulose is due to direct heat decomposition.[43] While between 330 and 485°C, the third stage of breakdown

Table 2. Identification of peaks ATR-FTIR spectra of the *CM* fibers.

Wave number (cm^{-1})	Vibrations mode(s)	Source(s)	References
3350	O–H stretching	Cellulose, Hemicelluloses	32
2884	C–H stretching	Cellulose, Hemicelluloses	33
1650–1600	C=O stretching	Hemicelluloses, lignin and extractives	34
1500	H–O–H bending of absorbed water	Water	33
1456–1417	H–C–H bending of absorbed water	Cellulose	35
1370–1324	C–H stretching	Lignin compounds	32
1230	-COO stretching	Hemicelluloses	36
1153	C–O bridge stretching	Cellulose	37
1029	C–O–C bridge stretching	Cellulose, Hemicelluloses	38
897	ß-glycosidic linkage	Cellulose, hemicelluloses	38

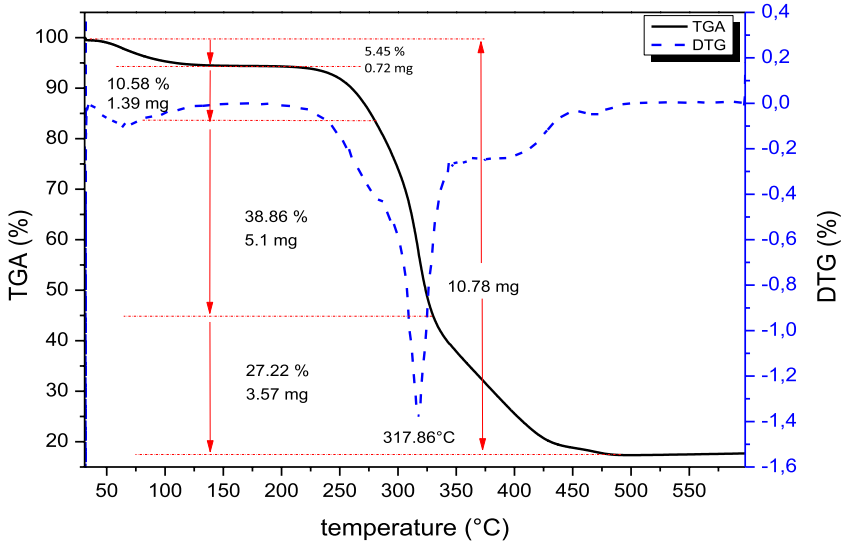

Figure 5. ATG/DTG curves of the *CM* fibers.

occurs, with a residual yield of 27.22%. Table 3 shows the thermal stability and degradation data for different natural fibers compared to previous studies. *CM* fibers can be safely employed as reinforcement for polymer reinforced composites at working temperatures below 210°C, according to the aforementioned analysis.

XRD

The crystalline structure of the fiber can be determined by the XRD technique. The XRD pattern of *CM* fibers is shown in Figure 6. In *CM*, I_{am} denotes the amorphous component and I_{002} represents the crystalline part of the particles.[29] The crystallinity index for *Centaurea Melitensis* fiber was calculated using the relationship (2), and it was found to be 47.69%, compared to *Cissus vitiginea stem* fiber (30.5%), *Momordica charantia* (21.42%), *Cereus Hildmannianus* (40.19%), *Vachelia farnesiana* (13%), *Cardiospermum Halicababum* (32.21%), and *Silybum marianum* (45%), less of *Kigelia africana* (57.38%), and *Areca catechu L* (55.5%). The higher index is due to improvements in cellulose chain packing, disruption of hydrogen bonds, elimination of amorphous components and non-cellulose materials, reorganization of crystalline regions, and water loss.[46] The average size of a single crystal is defined as crystallization size (CS), which was estimated at 16.92 nm for *Centaurea Melitensis* using equation (4). *Centaurea Melitensis* fibers have a CS value comparable to *Kigelia africana* (1.73 nm), *Cissus vitiginea* stem (12.69 nm) fibers, and

Table 3. Temperature of degradation and thermal stability of *CM* fiber in compared to other types of natural fibers.

Fibers type	T (°C)	W/m loss (%)	T (°C)	W/m loss (%)	T (°C)	W/m loss (%)	TS[a] (° C)	TD[b] (°C)	RW[c] (%)	References
Centaurea Melitensis	42–150	5.45	210–280	10.58	280–330	38.86	210	317.86	27.22	Present work
Kigelia africana	40–150	9.23	212–365	70	365–620	79.64	212	340	1.127	10
Cissus vitiginea stem	83	—	257	—	500	52.5	200	304	16	11
Momordica charantia	102	—	140–225	15.5	255–369	36.43	250	339.1	21	12
Cereus Hildmannianus	127.3	1.74	285.9	12.93	285.9–356.7	46.83	285.9	356.7	26.71	13
Vachellia farnesiana	30–110	9.7	165–240	14.5	270–361	36	—	324	28.71	14
Cardiospermum Halicababum	115	8.314	163–240	5.146	267–373	39.364	—	336	32.16	15
Silybum marianum	130.40	7.76	225–400	55.92	400–600	9.13	225	357.72	27	16
Areca catechu L	80	8.47	240–350	47.66	350–549.5	15.46	240	325.8	28.41	17

[a]Thermal stability.
[b]Thermal Degradability.
[c]Residual weight.

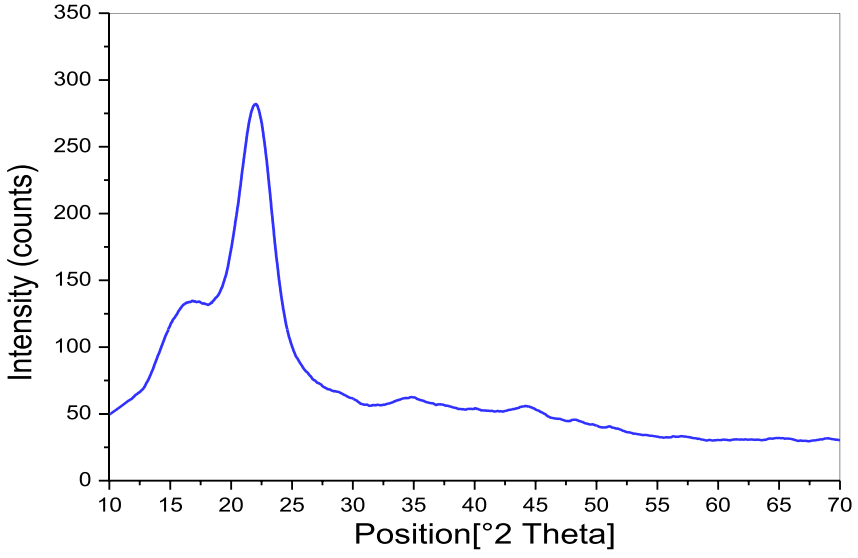

Figure 6. X-ray spectra of the *CM* fibers.

Areca catechu L (7.9 nm), and lower than *Cereus Hildmannianus* fibers (28.27 nm), *Vachellia farnesiana* fibers (31.89 nm), and *Cardiospermum Halicababum* fibers (29.77 nm). Table 4 gives a comparative assessment of the crystal characteristics of various different natural fibers.

Mechanical test

Mechanical properties play a critical role in deciding the use of natural fibers in various structural applications. Figure 7 shows the stress-strain curve of *CM* fibers. Where the value of the tensile strength of the fiber *Centaurea Melitensis* is 336.87 ± 59.94 MPa. We note here that this strength is less than *Cereus Hildmannianus* (2650.19 ± 42 MPa), and is approximately equal to that of the fiber *Areca catechu L* (322.829 ± 67 MPa), and is higher than that of the fiber *Kigelia africana* (52.68 ± 11.97 MPa), *Cissus vitiginea stem* (304.43 ± 35 MPa), *Momordica charantia* (36.5 ± 1.04 MPa), *Vachellia farnesiana* (33.075 ± 1.3 MPa), *Cardiospermum Halicababum* (20.7 ± 1.0 MPa), and *Silybum marianum* (201.16 MPa). The brittle nature of the material causes the rapid breakdown of the fibers a result of the main components such as lignin and hemicelluloses. The values of Strain at failure and Young's modulus

Table 4. Comparison of crystalline parameters from XRD of *CM* fibers.

Fibers type	Peak position (°)	FWHM	Area (%)	Crystalline index (%)	Crystallite size (nm)	References
Centaurea Melitensis	16.86 22	5.52 4.11	316.48 909.26	47.69	16.92	Present work
Kigelia africana	—	—	—	57.38	1.73	[10]
Cissus vitiginea stem	—	—	—	30.5	12.69	[11]
Momordica charantia	16.12 21.91	—	—	21.42	—	[12]
Cereus Hildmannianus	14.28 23.71	—	—	40.19	28.27	[13]
Vachellia farnesiana	15.24 22.59	—	—	13	31.89	[14]
Cardiospermum Halicababum	14.90 21.83	—	—	32.21	29.77	[15]
Silybum marianum	18.25 21.99	—	—	45	—	[16]
Areca catechu L	20.12	—	—	55.5	7.9	[17]

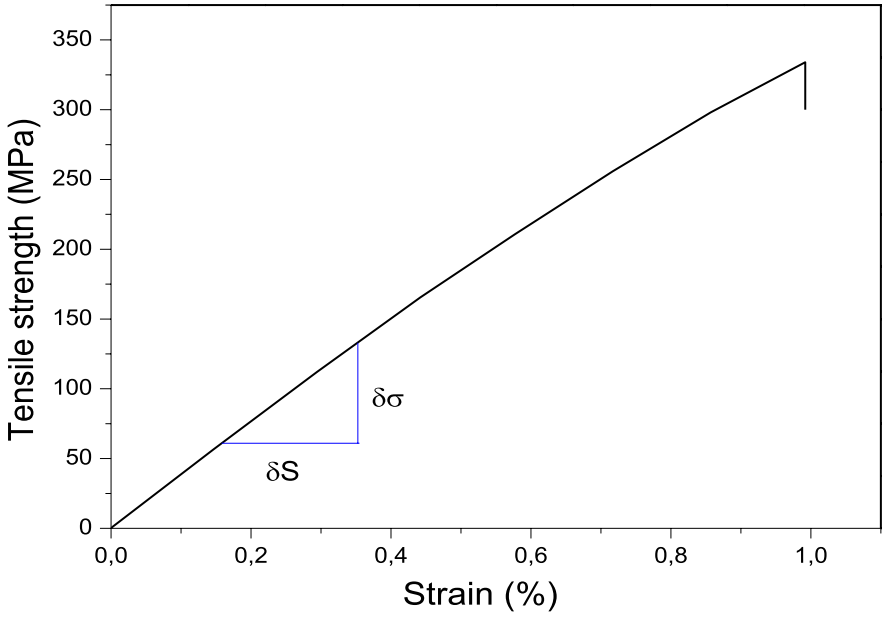

Figure 7. Typical tensile stress strain curve for *CM* fibers.

for *Centaurea Melitensis* fibers is 23.87 ± 5.21 GPa and 1.27 ± 0.36%, respectively. Table 5 represents the mechanical properties of *CM* fibers and their comparison with other natural fibers that were recently studied.

Figure 8 represents the distribution of Young's modulus and tensile strength in terms of fiber diameter *CM*. Through this contrast the mechanical properties of *CM* fibers can be evaluated. We notice a decrease in Young's modulus and tensile strength as the diameter of the fibers increases. This is associated with the rate at which non-cellulosic components rise with fiber diameter and lumen diameter.[29] Young's modulus and tensile strength values are also noted to be scattered due to a variety of random variables such as test conditions, varying number of fibroblast walls, as well as age, area, and method of extraction. With increasing diameter, Young's modulus and tensile strength decrease and this is due to the diameter, number and size of the lumen in the fibroblasts.[10] It was also noted that these results are consistent with the natural fibers that have been studied by other researchers in.[24,29,47]

WEIBULL statistical

The Weibull analysis can also used to quantify the variation of the probabilistic strength of fibers. Figure 9 shows 2 and 3-parameter Weibull distributions for stress, Young's modulus, and strain at failure. These distributions describe the mechanical characteristics arising from the experimental findings of *CM* fibers In order to determine the most suitable distribution. The linear equation (LS estimation of least squares) is used to graphically determine the coefficient (m) for the 2 and three parameters, which is represented by the slope of the curve. It is clear that the experimental data correctly fit the Weibull distribution and are rather near to the line. The modulus (m) and (σ_0) strain characteristic of Weibull

Table 5. Mechanical properties of *CM* fiber in comparison with other cellulose-based natural fibers.

Fibers type	Tensile strength (MPa)	Young's modulus (GPa)	Strain at failure (%)	References
Centaurea Melitensis	336.87 ± 59.94	23.87 ± 5.21	1.27 ± 0.36	Present work
Kigelia africana	52.68 ± 11.97	36.01 ± 33.68	0.22 ± 0.11	10
Cissus vitiginea stem	304.43 ± 35	5.85 ± 1.10	8.92 ± 1.4	11
Momordica charantia	36.5 ± 1.04	—	—	12
Cereus Hildmannianus	2650.19 ± 42	2.12 ± 0.3	1.3 ± 0.7	13
Vachellia farnesiana	33.075 ± 1.3	—	2.3 ± 0.1	14
Cardiospermum Halicababum	20.7 ± 1.0	—	2.1 ± 0.12	15
Silybum marianum	201.16	15.97	1.593	16
Areca catechu L	322.829 ± 67	3.155 ± 2.31	10.23 ± 2.75	17

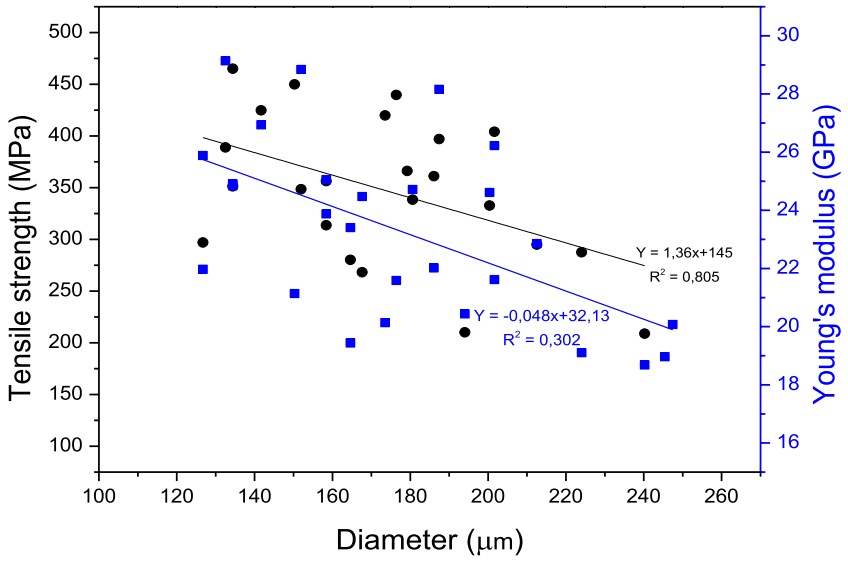

Figure 8. Young's modulus and tensile strength as a function of fiber diameter.

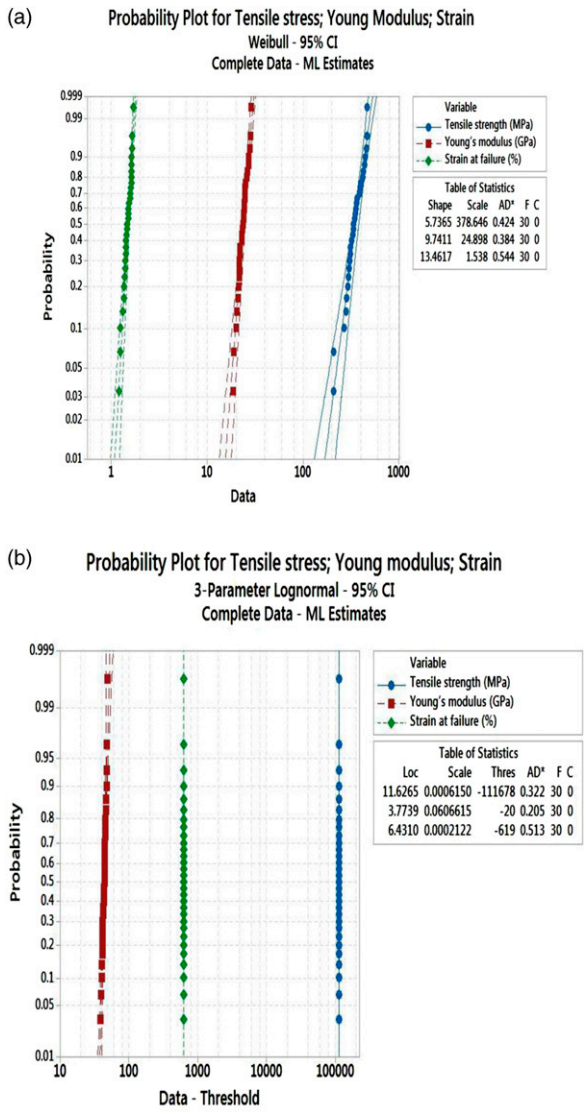

Figure 9. Weibull distribution for tensile strength, young's modulus, and strain at failure of *CM* fibers: (a) two parameter, (b) three-parameter.

with two parameters of *CM* fibers are 5.73 and (σ_0) are estimated at 378.64 MPa, respectively. For the three-parameter Weibull method, we find that (m) is estimated at 11.62 and (σ_0) is estimated at 0.0006 MPa, respectively. The study of the findings reveals that a two-parameter Weibull distribution is the best suitable approach in our case since the mean strength estimations for *CM* fibers generated by this method are the closest to those obtained experimentally and estimated as 336.87 MPa. However, the value of Young's modulus (E_0) and strain at failure (ε_0) was found by distributing two-parameters Weibull, which is also the closest to the experimentally obtained, estimated at 24.89 GPa and 1.53%, respectively. It is evident that the two-parameter Weibull distribution enables the values of mechanical characteristics to be very near to the average of the values discovered via experimentation.

Micro-droplet test

Micro-droplet test is a method that is used to measure interfacial shear strength between fiber and matrix. This

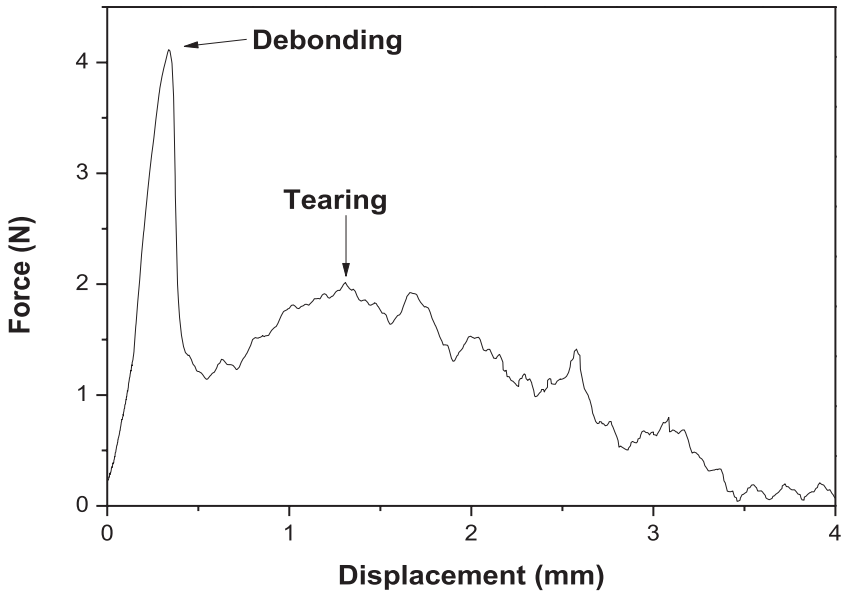

Figure 10. Force–displacement curve for droplet debonding.

Table 6. comparison of IFSS shear stress results for *CM* fibers with other fibers.

Fiber/matrix	IFSS(MPa)	References
CM/epoxy	9.82 ± 2.35	Present work
Inula viscosa/epoxy	3.22 ± 0.47	[48]
Pineapple/PHBV*	8.23	[52]
Glass/epoxy	38	[53]
Kevlar/phenol-ormaldehyde	23.5	[54]
Basalt/epoxy	11.4 ± 3.1	[55]
Glass/polyester	15.7±2.9	[56]

*poly (hydroxybutyrate-co-valerate).

section calculated the interface strength between *CM* fiber and epoxy resin by the droplet test. The apparent shear stress IFSS was won from the test results. Figure 10 represents the force/displacement curve of the *CM* fiber, It is remarkable that the apparent bond strength measured with micro-drop tests varies widely. There are many factors that cause this discrepancy, among which are the increase in the roughness and surface area of the fibers, the length of the immersed resin and the different diameters of the fibers, which leads to the effect of mechanical cross linking between the fibers and the composite matrix.[48] The average IFSS for fiber-epoxy matrix combination is 9.82 ± 2.35 MPa. Table 6 shows the comparison of IFSS shear stress results for *CM* fibers with other fibers. We can say that the results obtained are close compared to the results of previous studies such as, *Inula viscosa fibers,*[48] *Pineapple fibers,*[49] *Glass fibers,*[50] *Kevla fibers,*[51] *basalt fibers,*[52] *Glass fibers,*[53] *Agave sisalana fibers*.[54]

Scanning electron microscopy

The SEM was used to examine the surfaces morphologies of the fiber, generally after fracture, and can provide a very close view of the longitudinal section and transverse surface. Figure 11 represents the SEM micrographs of the *CM* fibers in longitudinal section and transverse surface, and is a suitable method for verifying the morphology of the fibers. Figure 11(a) shows the longitudinal width of the fibers, which shows wavy patterns due to the irregular diameter of the individual fibers. As shown in Figure 11(b), the surface morphology of the fibers shows the presence of bumps and inclusions along the surface of the fibers, which helps in better bonding of the fibers with the polymer matrix.[34] On the other hand, Figure 11(c) shows that *CM* fibers consist of cellular primary fibrils that are linked to each other by lignin and hemicelluloses, which contributes to the surface roughness of the fibers, which leads to better adhesion to the matrix.[55] The transverse image of the *CM* fiber is shown in Figure 11(d) and (e). From Figure 11(d) we notice that the *CM* fibers have an oval shape which is an important factor for composite applications.[56] Furthermore, Figure 11(e) shows the spaces between the cell fibers represented by a central orifice called the lumen. The difference in the size and shape of the cellular fibers also shows an irregularity in the diameter of the fibers, which affects the mechanical properties of the *CM* fibers. Where the diameter of the cell fibers of *CM* is estimated

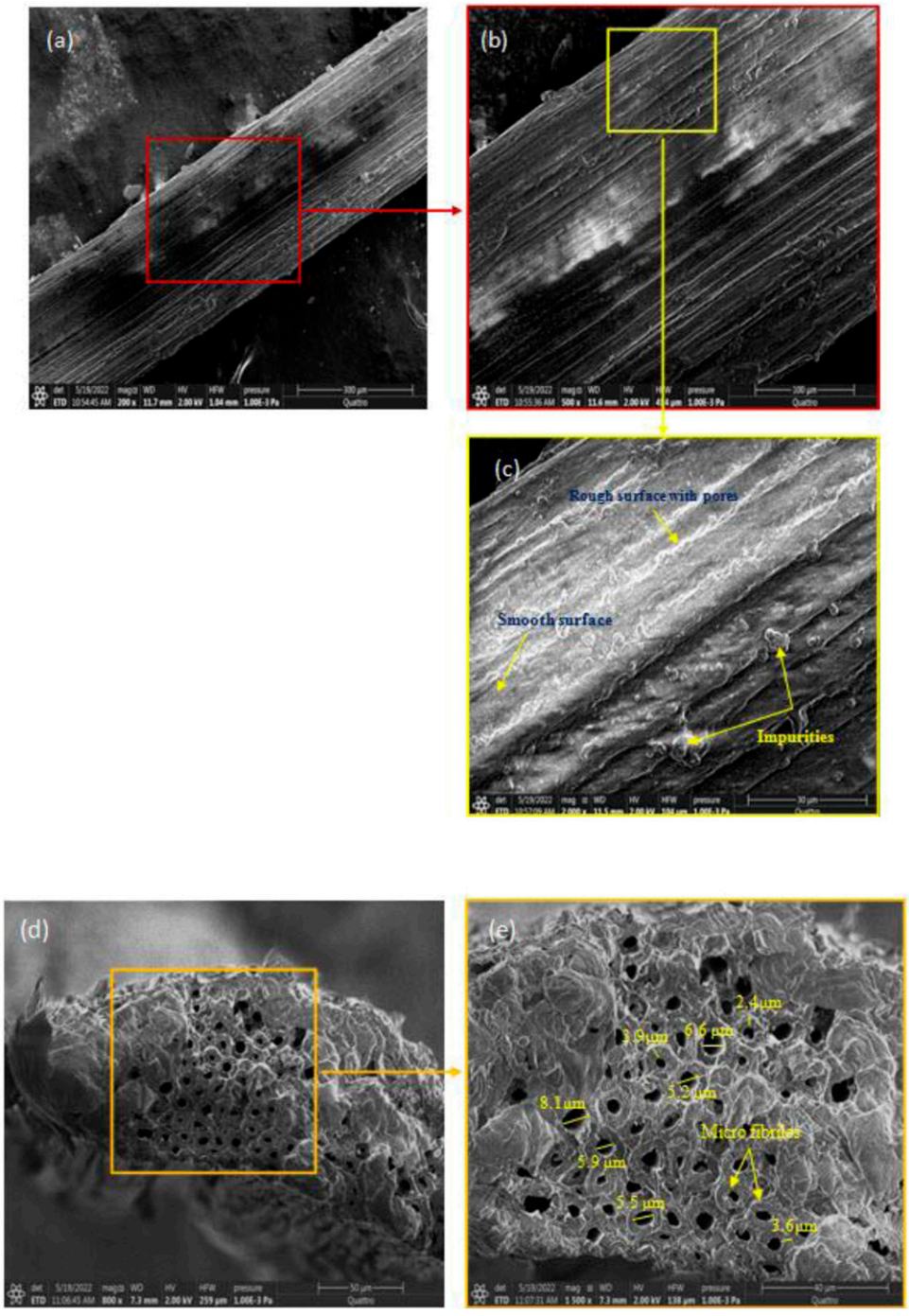

Figure 11. Scanning electron microscopy micrographs of *CM* fibers.

in 6.26 ± 1.84 μm while the thickness of the wall is in 3.3 ± 0.9 μm.

Conclusion

In this research paper, the new extracted fiber from *Centaurea Melitensis* plant, which is abundant and cost-effective, has been characterized and studied. For this purpose, the morphological, chemical, physical and mechanical properties have been examined. Based on the conducted analysis and the corresponding findings, the density of *Centaurea Melitensis* fibers has been determined to be 1.269 ± 0.018 g/cm^3, which allows to conclude its benefits in using it in lightweight composite materials. It has been observed using SEM the presence of protrusions in the fibers that allow adherence to the polymer matrix. By performing TGA analysis, the thermal stability of the fibers been found to be up to 210°C, which considerably helps to use them at high temperature for the polymer matrix to manufacture the composite. Also, FTIR and XRD analysis proved the presence of major components such as cellulose, hemicelluloses and lignin with crystallization index of 47.69% and crystal size of 16.92 nm. In addition, the mechanical properties showed that the value of the tensile strength of the fibers, Young's modulus and strain at failure are 336.87 ± 59.94 MPa, 23.87 ± 5.21 GPa, 1.27 ± 0.36%, respectively. Micro-droplet tests also proved that the value of the interfacial shear strength between the fibers and the matrix is 9.82 ± 2.35 MPa. From obtained results and as a main conclusion of this paper is that *Centaurea Melitensis* fibers are very suitable for use as reinforcement in polymer-reinforced composites.

Declaration of conflicting interests

The author(s) declared no potential conflicts of interest with respect to the research, authorship, and/or publication of this article.

Funding

The author(s) received no financial support for the research, authorship, and/or publication of this article.

ORCID iD

Mansour ROKBI https://orcid.org/0000-0001-5856-662X

References

1. Porras A, Maranon A and Ashcroft I. Characterization of a novel natural cellulose fabric from Manicaria saccifera palm as possible reinforcement of composite materials. *Composites B: Eng* 2015; 74: 66–73.
2. Lee K, Kelly D and Kennedy G Jr. Pulmonary response to inhaled Kevlar aramid synthetic fibers in rats. *Toxicol Appl Pharmacol* 1983; 71(2): 242–253.
3. Rapisarda V, Loreto C, Ledda C, et al. Cytotoxicity, oxidative stress and genotoxicity induced by glass fibers on human alveolar epithelial cell line A549. *Toxicol Vitro* 2015; 29(3): 551–557.
4. Indran S and Raj RE. Characterization of new natural cellulosic fiber from Cissus quadrangularis stem. *Carbohydr Polymers* 2015; 117: 392–399.
5. Senthamaraikannan P and Kathiresan M. Characterization of raw and alkali treated new natural cellulosic fiber from Coccinia grandis.L. *Carbohydr Polym* 2018; 186: 332–343.
6. Ganapathy T, Sathiskumar R, Senthamaraikannan P, et al. Characterization of raw and alkali treated new natural cellulosic fibres extracted from the aerial roots of banyan tree. *Int J Biol Macromol* 2019; 138: 573–581.
7. Ramesh M, Palanikumar K and Reddy KH. Mechanical property evaluation of sisal–jute–glass fiber reinforced polyester composites. *Composites B Eng* 2013; 48: 1–9.
8. Kumar KP and Sekaran ASJ. Some natural fibers used in polymer composites and their extraction processes: a review. *J Reinf Plast Compos* 2014; 33(20): 1879–1892.
9. Manimaran P, Saravanan S, Sanjay M, et al. Characterization of new cellulosic fiber: dracaena reflexa as a reinforcement for polymer composite structures. *J Mater Res Technol* 2019; 8(2): 1952–1963.
10. Siva R, Valarmathi T, Palanikumar K, et al. Study on a Novel natural cellulosic fiber from Kigelia africana fruit: characterization and analysis. *Carbohydr Polym* 2020; 244: 116494.
11. Chakravarthy S, S M, Raju JSN, et al. Characterization of novel natural cellulosic fiber extracted from the stem of Cissus vitiginea plant. *Int J Biol Macromol* 2020; 161: 1358–1370.
12. Khan A, Raghunathan V, Singaravelu DL, et al. Extraction and characterization of cellulose fibers from the stem of momordica charantia. *J Nat Fibers* 2020; 19: 1–11.
13. Subramanian SG, Rajkumar R and Ramkumar T. Characterization of natural cellulosic fiber from cereus hildmannianus. *J Nat Fibers* 2021; 18(3): 343–354.
14. Vijay R, James Dhilip JD, Gowtham S, et al. Characterization of natural cellulose fiber from the barks of vachellia farnesiana. *J Nat Fibers* 2020; 19: 1–10.
15. Vinod A, Vijay R, Singaravelu DL, et al. Extraction and characterization of natural fiber from stem of cardiospermum halicababum. *J Nat Fibers* 2021; 18(6): 898–908.
16. Laifa F, Rokbi M, Amroune S, et al. Investigation of mechanical, physicochemical, and thermal properties of new fiber from Silybum marianum bark fiber. *J Compos Mater* 2022; 56: 00219983221090020.
17. Binoj J, Raj RE, Sreenivasan VS, et al. Morphological, physical, mechanical, chemical and thermal characterization of sustainable Indian areca fruit husk fibers (Areca catechu L.) as potential alternate for hazardous synthetic fibers. *J Bionic Eng* 2016; 13(1): 156–165.

18. Balaji A and Nagarajan K. Characterization of alkali treated and untreated new cellulosic fiber from Saharan aloe vera cactus leaves. *Carbohydr Polymers* 2017; 174: 200–208.
19. Moroney JR and Rundel PW. Abundance and dispersion of the invasive Mediterranean annual, Centaurea melitensis in its native and non-native ranges. *Biol Invasions* 2013; 15(3): 495–507.
20. Lejeune KD and Seastedt TR. Centaurea species: the forb that won the west. *Conservation Biol* 2001; 15(6): 1568–1574.
21. Vila M and Weiner J. Are invasive plant species better competitors than native plant species?–evidence from pairwise experiments. *Oikos* 2004; 105(2): 229–238.
22. Widmer TL, Guermache F, Dolgovskaia MY, et al. Enhanced growth and seed properties in introduced vs. native populations of yellow starthistle (Centaurea solstitialis). *Weed Sci* 2007; 55(5): 465–473.
23. Keskin OY, Dalmis R, Balci Kilic G, et al. Extraction and characterization of cellulosic fiber from Centaurea solstitialis for composites. *Cellulose* 2020; 27(17): 9963–9974.
24. Mansour R, Abdelaziz A and Zohra AF. Characterization of long lignocellulosic fibers extracted from Hyphaene thebaica L. leaves. *Res J Textile Apparel* 2018; 22: 195–211.
25. Brahim SB and Cheikh RB. Influence of fibre orientation and volume fraction on the tensile properties of unidirectional Alfa-polyester composite. *Compos Sci Technol* 2007; 67(1): 140–147.
26. Msahli S, Ydrean J and Sakli F. Evaluating the fineness of Agave americana L. fibers. *Textile Research Journal* 2005; 75(7): 540–543.
27. Segal L, Creely J, Martin A, et al. An empirical method for estimating the degree of crystallinity of native cellulose using the X-ray diffractometer. *Textile Research Journal* 1959; 29(10): 786–794.
28. Miller B, Muri P and Rebenfeld L. A microbond method for determination of the shear strength of a fiber/resin interface. *Compos Sci Technol* 1987; 28(1): 17–32.
29. Belouadah Z, Ati A and Rokbi M. Characterization of new natural cellulosic fiber from Lygeum spartum L. *Carbohydr Polym* 2015; 134: 429–437.
30. Sreenivasan V, Somasundaram S, Ravindran D, et al. Microstructural, physico-chemical and mechanical characterisation of Sansevieria cylindrica fibres–An exploratory investigation. *Mater Des* 2011; 32(1): 453–461.
31. Belouadah Z, Rokbi M and Ati A. Manufacturing and characterization of new composite based on epoxy resin and Lygeum Spartum L. plant. *J Nat Fibers* 2022; 19(11): 4236–4248.
32. Belouadah Z, Belhaneche-Bensemra N, Ati A, et al. Characterization of ligno-cellulosic fiber extracted from Atriplex halimus L. plant. *Int J Biol Macromol* 2021; 168: 806–815.
33. Lemita N, Deghboudj S, Rokbi M, et al. Characterization and analysis of novel natural cellulosic fiber extracted from Strelitzia reginae plant. *J Compos Mater* 2022; 56(1): 99–114.
34. Indran S, Raj RE and Sreenivasan V. Characterization of new natural cellulosic fiber from Cissus quadrangularis root. *Carbohydr Polym* 2014; 110: 423–429.
35. Hossain MK, Dewan MW, Hosur M, et al. Effect of surface treatment and nanoclay on thermal and mechanical performances of jute fabric/biopol 'green'composites. *J Reinf Plast Compos* 2011; 30(22): 1841–1856.
36. Kovačević Z, Vukušić SB and Zimniewska M. Comparison of Spanish broom (Spartium junceum L.) and flax (Linum usitatissimum) fibre. *Textile Res J* 2012; 82(17): 1786–1798.
37. Jabbar A, Jiří M, Jakub W, et al. Tensile, surface and thermal characterization of jute fibres after novel treatments. *Indian J Fibre Text Res* 2016; 42: 249–254.
38. Kumar R, Meena AS, Chopra A, et al. Keratin gene expression differences in wool follicles and sequence diversity of high glycine-tyrosine keratin-associated proteins (kaps) in magra sheep of India. *J Nat Fibers* 2020; 17(9): 1257–1263.
39. Chikouche MDL, Merrouche A, Azizi A, et al. Influence of alkali treatment on the mechanical properties of new cane fibre/polyester composites. *J Reinf Plast Comp* 2015; 34(16): 1329–1339.
40. Sudha S and Thilagavathi G. Effect of alkali treatment on mechanical properties of woven jute composites. *J Text Inst* 2016; 107(6): 691–701.
41. Zannen S, Ghali L, Halimi MT, et al. Effect of chemical extraction on physicochemical and mechanical properties of doum palm fibres. *Adv Mater Phys Chem* 2014; 4(10): 203–216.
42. Subramanian K, Senthil Kumar P, Jeyapal P, et al. Characterization of ligno-cellulosic seed fibre from Wrightia Tinctoria plant for textile applications—an exploratory investigation. *Eur Polym J* 2005; 41(4): 853–861.
43. Manimaran P, Senthamaraikannan P, Sanjay M, et al. Study on characterization of Furcraea foetida new natural fiber as composite reinforcement for lightweight applications. *Carbohydr Polym* 2018; 181: 650–658.
44. Ridzuan M, Abdul Majid M, Afendi M, et al. Characterisation of natural cellulosic fibre from Pennisetum purpureum stem as potential reinforcement of polymer composites. *Mater Des* 2016; 89: 839–847.
45. Maache M, Bezazi A, Amroune S, et al. Characterization of a novel natural cellulosic fiber from Juncus effusus L. *Carbohydr Polym* 2017; 171: 163–172.
46. Reddy KO, Uma Maheswari C, Shukla M, et al. Tensile and structural characterization of alkali treated Borassus fruit fine fibers. *Compos B Eng* 2013; 44(1): 433–438.
47. Bezazi A, Belaadi A, Bourchak M, et al. Novel extraction techniques, chemical and mechanical characterisation of Agave americana L. natural fibres. *Compos B Eng* 2014; 66: 194–203.
48. Moussaoui N, Rokbi M, Osmani H, et al. Extraction and characterization of fiber treatment Inula viscosa fibers as potential polymer composite reinforcement. *J Polym Environ* 2021; 29(11): 3779–3793.
49. Luo S and Netravali A. Interfacial and mechanical properties of environment-friendly "green" composites made from pineapple fibers and poly (hydroxybutyrate-co-valerate) resin. *J Mater Sci* 1999; 34(15): 3709–3719.

50. Wu H. A comparison of micromechanical evaluation on interfacial shear strength using microbond pull-out and micro-indentation tests. *J Mater Sci Lett* 1997; 16(24): 2039–2040.
51. Gopal P, Dharani LR, Subramaniam N, et al. 'Bundle-debond'technique for characterizing fibre/matrix interfacial adhesion. *J Mat Sci* 1994; 29(5): 1185–1190.
52. Ciniņa I, Zīle O and Andersons J. Predicting the tensile strength of A UD basalt/epoxy composite used for the confinement of concrete structures. *Mech Compos Mater* 2013; 48(6): 611–618.
53. Baley C, Grohens Y, Busnel F, et al. Application of interlaminar tests to marine composites. Relation between glass fibre/polymer interfaces and interlaminar properties of marine composites. *Appl Compos Mater* 2004; 11(2): 77–98.
54. Towo AN, Ansell MP, Pastor ML, et al. Weibull analysis of microbond shear strength at sisal fibre–polyester resin interfaces. *Compos Interf* 2005; 12(1-2): 77–93.
55. Kılınç AÇ, Koktas S, Seki Y, et al. Extraction and investigation of lightweight and porous natural fiber from Conium maculatum as a potential reinforcement for composite materials in transportation. *Compos B Eng* 2018; 140: 1–8.
56. Bezazi A, Amroune S, Scarpa F, et al. Investigation of the date palm fiber for green composites reinforcement: Quasi-static and fatigue characterization of the fiber. *Ind Crops Prod* 2020; 146: 112135.